On the influence of solution and ageing treatments on the microstructure of ZK40 alloys modified with Ca, Gd, Nd and Y additions

Ricardo Henrique Buzolin[1,2a], Dr. Chamini Lakshi Mendis[1,3,b], Dr. Domonkos Tolnai[1,c], Dr. Erenilton Pereira da Silva[4,d], Prof. Karl Ulrich Kainer[1,e], Dr. Norbert Hort[1,f], Prof. Haroldo Cavalcanti Pinto*[5,g]

[1]*Magnesium Innovation Centre, Helmholtz-Zentrum Geesthacht, Max-Planck-Strasse 1, D 21502, Geesthacht, Germany*

[2]*Institute of Materials Science, Joining and Forming, Graz University of Technology, Kopernikusgasse 24/I, 8010 Graz, Austria*

[3]*Brunel Centre for Advanced Solidification Technology, Brunel University London, Uxbridge, Middlesex, UB8 3PH, UK*

[4]*Department of Materials Engineering, Federal University of Sao Carlos, Rodovia Washington Luís (SP-310) Km 235, 13563-120, Sao Carlos, Brazil*

[5]*Department of Materials Engineering, University of Sao Paulo, Av. Joao Dagnone, 1100 Jd. Sta Angelina, 13563-120, Sao Carlos, Brazil*

[a]*ricardo.buzolin@tugraz.at*, [b]chamini.mendis@brunel.ac.uk, *cdomonkos.tolnai@hzg.de*, [d]*erenilton.silva@sc.usp.br*, [e]karl.kainer@hzg.de, [f]norbert.hort@hzg.de, [g]*haroldo@sc.usp.br (corresponging author)*

Keywords: Magnesium alloys, heat treatment, solution treatment, rare earth, calcium oxide, ageing, Zn-Zr precipitates

Abstract

As-cast ZK40 alloys, modified with the addition of CaO, Gd, Nd and Y were investigated. Solution heat treatments were performed based on differential thermal analysis results. The unmodified ZK40 alloy exhibited microstructure with nearly no intermetallic compound but with precipitates formed during the solution treatment. The modified ZK40 alloys exhibited a semi-

dissolved network of intermetallic compounds along the grain boundaries and zones of intermetallic compounds within the grains. Interestingly, no precipitates were observed immediately next to the grain boundaries. The energy dispersive X-ray spectroscopy~~EDXS~~ line scans show an enrichment of Zn and Zr in the regions where the precipitates are found, suggesting that they are Zn-Zr precipitates. The ageing behaviour was compared between the as-cast and the solution treated materials and it was found that apart from the ZK40-Gd, ZK40-Nd and ZK40-Y aged at 200 °C after solution treatment, there is no notable ageing response for the investigated alloys.

Introduction

Mg alloys have a high potential for use as lightweight structural materials due to the satisfactory strength/weight ratio. However, obstacles such as low corrosion resistance and the poor absolute strength impede the use of magnesium alloys [1]. The control of the microstructure and the understanding of the effect of its components on~~in~~ the materials properties are of importance in order to design high performance Mg alloys.

Zn is a widely used alloying element for Mg alloys due to the low cost and the improvement of strength properties of both cast and wrought alloys [2]. Mg-Zn alloy shows promising age-hardening response in comparison to other Mg systems [3]. Among the investigated Mg alloy systems, ZK alloys are one of the highest strength cast alloys available commercially [4]. The mechanical properties [5], microstructure modification [6], and texture randomisation [7,8] caused by Ca additions were previously investigated. The addition of Ca to Mg-Zn alloys refines the grain size, contributes to solid solution hardening and enhances the precipitation hardening response [9,10]. Wiese *et al.* [11] showed that CaO reduces to form MgO and Mg_2Ca during casting and solidification, which can provide an easier route to add Ca to Mg alloys. The formation of thermally stable secondary phases that stabilizes the microstructure during heat treatments and thermo-mechanical processes is of interest for applications at elevated temperatures [12].

Investigations on the effect of rare earth elements (RE)~~RE~~ addition on Mg alloys are~~is~~ extensive. Mg alloys with RE addition show potential for achieving improved strength and creep resistance compared with the AZ system and the most notable ones are based on the Mg-Gd, Mg-Gd-Y, Mg-Gd-Nd, and Mg-Y-Nd systems [13,14,15,16,17,18]. The role of Y in Mg based alloys has been studied extensively. Y is considered to be one of the most effective alloying additions which improves the mechanical properties at high temperatures for Mg alloys [19,20,21,22]. The addition of Zn to Mg alloys containing Y has significantly improved creep strength and it is proposed that Zn suppresses the non-basal slip through the formation of planar defects [23,24]. The addition of Zn to a Mg-Nd-Zr alloy [25] increased the strength and decreased the plasticity at all test temperatures from ambient to 250 °C. However, strengthening caused by the Zn addition decreases with rising temperature. The effect of the Zn on the mechanical properties of ~~a~~ Mg-Gd-Y-Zr alloy was investigated previously [26]. Although the addition of Zn degrades the age-hardening response, the maximum tensile elongation is enhanced by discontinuous precipitation of a 14H-type long period stacking order (LPSO) phase at grain boundaries and with grains in the over-aged condition~~, which enhances the maximum tensile elongation~~. Furthermore, ~~T~~the addition of Gd to a ZK60 alloy led to a reduction of the age-hardening response [27].

This work aims to investigate the impact of solution heat treatment on the ageing response and microstructure features of ZK40 alloys modified with individual RE and CaO additions.

Experimental procedure

Five alloys (ZK40, ZK40-CaO, ZK40-Gd, ZK40-Nd and ZK40-Y) were prepared with pure Mg, Zn, CaO, Nd and master alloys Mg 10 wt.% Y, Mg 4 wt.% Gd and Mg-33 wt.%Zr (Zirmax®). Mg was molten in an electric resistance furnace at 750 °C and alloying elements were added to the melt and stirred for 10 min. The melt was then poured into a preheated thin walled steel mould held at 660 °C for 15 min. Then, the mould was immersed into water at a rate of 10 $mm.s^{-1}$ until the top of the melt was in line with the cooling water. The ingots had a bottom diameter of 250 mm and the height of 300 mm. The indirect casting procedure was adopted

to provide a homogeneous microstructure. Table1 shows the actual compositions of the alloys prepared for this investigation measured with X-ray fluorescence (Zn and Gd) and spark analyser (Ca, Cu, Fe, Nd, Ni, Y, Zr).

Differential Thermal Analysis (DTA) was conducted using a Mettler Toledo DTA model SDTA 851 under an Ar atmosphere in a steel crucible at heating and cooling rates of 10 K/min in the temperature range of 300-700 °C. The heating and cooling cycles were repeated at least three times for each sample to ensure reproducibility of the measurement. The DTA data was then used to provide the appropriate temperatures for solution treatments of the investigated alloys.

Solid ~~S~~solution heat treatments were performed using and electric resistance furnace under ~~an~~ Ar protective atmosphere for a holding time of 24 h. The solution treatment temperature varied from alloy to alloy and for the ZK40-Gd and ZK40-Nd two temperatures were selected as listed in Table 2.

Ageing treatment were performed for the as-cast material (T5) and for the solution treated material (T6). In the case of the ZK40-Gd and ZK40-Nd, in which two solution treatment temperatures were investigated, the material treated at highest temperature was chosen, i.e., ZK40-Gd solution treated at 475 °C for 24 h and ZK40-Nd solution treated at 475 °C for 24 h. An oil bath furnace working with silicon-based oil was used to perform the ageing treatments. Three different temperatures were selected: 150 °C, 175 °C and 200 °C. Hardness measurements were performed to evaluated the hardness evolution during ageing. Vickers hardness were measured using an applied load of 5 kg for a holding time of 30 s.

Specimens for metallographic characterisation were ground with SiC abrasive papers from P500 to P2500, followed by polishing with OPS. Scanning electron microscopy (SEM) was conducted on the unetched samples using a Carl Zeiss FEG-SEM Ultra 55 and a FEI Inspect F-50. Stereological measurements of the area fraction of intermetallic compounds were performed by using a minimum of 10 random BSE (backscattered electron) macrographs and were analysed using ImageJ software. The SEMs were equipped with e~~E~~nergy d~~D~~ispersive

X-ray sSpectrometers (EDXS)(EDXS) and EDXSEDXS line scans were recorded across the length of the grains to determine the elemental distribution. A Savitzky-Golay [28] filter with 20 points of window and a 4-degree polynomial was applied to smooth the EDXSEDXS lines scans.

Results and discussion

The DTA results show an exothermic peak during cooling from 700 °C at 636-638 °C attributed to the formation of α-Mg. Table 3 summarizes the peak temperatures for the formation of the intermetallic phase obtained by DTA (the plots are not presented here). For the ZK40-Nd alloy two peaks were detected. For the formation of α-Mg, the peak temperature during cooling was observed at 636-638 °C for the investigated alloys.

The SEM micrographs of the as-cast materials are shown in Figure 1 and illustrate the volume fraction and distribution of the intermetallic particles. The volume fraction of second phases is 1.6 ± 0.5%, 6.5 ± 0.9%, 5.7 ± 1.0%, 7.3 ± 0.6% and 3.1 ± 0.5% for ZK40, ZK40-CaO, ZK40-Gd, ZK-Nd and ZK40-Y, respectively. In the unmodified ZK40 alloy, discrete particles of intermetallic phase were observed randomly at triple points, and grain boundaries and within the grains. In addition, segregation of Zn was observed from the centre of grains to the intermetallic area as illustrated by the brighter regions close to the grain boundaries. The ZK40-CaO, ZK40-Gd, ZK40-Nd and ZK40-Y alloys contain a semi-continuous distribution of intermetallic particles along the grain boundaries. In the ZK40-CaO and the ZK40-Nd the interconnectivity is larger than the other alloys.

Figure 2 exhibits the microstructure of the solution heat treated ZK40 alloy at 320 °C for 24 h. The discrete intermetallic compounds are partially dissolved. However, precipitates at the grain boundaries as well as small precipitates in the α-Mg matrix are observed when analysing in higher magnification (Region A highlighted in Figure 2a), Figure2b.

The microstructure of the solution heat treated ZK40-CaO is shown in Figure 3. Comparing Figure3a with Figure1b, the main differences in the microstructure are the presence of a

precipitation zone within the grain for the solution heat treated ZK40-CaO alloy as well as a discontinuous network with dissociated parts of intermetallic compounds along the grain boundaries as a result of the partial dissolution during solution heat treatment. Figure3b highlights the size and distribution of the precipitates that are formed during solution treatment at 370 °C for 24 h for the ZK40-CaO alloy.

Figure 4 exhibits the microstructure of the solution heat treated ZK40-Gd alloy. Figure 4(a-c) exhibits the microstructure of the alloy for the solution treatment performed at 445 °C for 24 h and Figure 4(d-f) for the solution treatment performed at 475 °C for 24 h. Similar to the ZK40-CaO, the solution heat treated microstructure of the Zk40-Gd exhibited a discontinuous and partially dissolved network of intermetallic compounds along the grain boundaries and precipitates within the grains. However, one main difference compared to the ZK40-CaO is the presence of two different precipitates zones with different precipitate size, distribution and orientation. Figure 4(b,c) highlights the regions containing precipitates for the solution treatment carried at 445 °C for 24 h. The region closer to the grain boundary (Region C) is shown in Figure 4b, whereas the~~an~~ inner region (~~/~~Region D) as~~is~~ shown in Figure 4c. The distribution of the precipitates seems to be sparser in Region C compared to Region D. The microstructure of the ZK40-Gd heat treated at 475 °C for 24 h also exhibits two different precipitate zones. Interestingly, the inner region (Region F, Figure 4f) seems to have coarser precipitates and more sparsely distributed compared to region closer to the grain boundary (Region E, Figure 4e), which is nearly the opposite tendency showed for the heat treatment performed at 445~~0~~ °C for 24 h.

The microstructure of the ZK40-Nd after solution treatment (Figure 5) also exhibited comparable microstructure to the other modified ZK40 alloys. Figure 5(a,b) ~~exhibits~~ shows the microstructure of the ZK40-Nd after solution treatment at 440 °C for 24 h. A partially dissolved and discontinuously distributed network of intermetallic compounds along the grain boundaries is observed. Only one characteristic region of precipitates was found, Region G shown in Figure 5b. However, a slightly modified microstructure is found after solution

treatment at 475 °C for 24 h for the ZK40-Nd alloy. The network of intermetallic compounds seems to be dissolved, and intermetallic particles were formed at the grain boundaries. Two regions of precipitates are found for this alloy at this condition: Region H (Figure 5d) and I (Figure 5e). Comparable to the ZK40-Gd after solution treatment at 475 °C for 24 h, the inner region exhibited coarser and sparser distributed precipitates, and the region close to the grain boundary exhibited finer and more densely distributed precipitates.

Figure 6 ~~exhibits~~ shows the microstructure of the ZK40-Y after solution treatment at 480 °C for 24 h. Partial dissolution of the intermetallic compounds is observed and two characteristic regions of precipitates are found: Region K shown in Figure 6b and Region J shown in Figure 6c. The region closer to the grain boundary (Region J) exhibits finer precipitate compared to the middle of the grain (Region K).

In order to investigate the possible segregation of chemical elements after solution heat treatments, EDXS~~EDXS~~ line scans were measured and are shown in Figure 7. An enrichment of Zn and Zr within the grains is observed. A notable enrichment of Zn and Zr are observed in the regions containing precipitates in the case of the ZK40-Gd heat treated at 475 °C for 24 h and ZK40-Nd heat treated at 440 °C for 24 h. Zn-Zr precipitates are reported to be formed after solution treatment for a Mg-2Re-2Zn-0.8Ca-0.5Zr (wt.%) [29], Mg-Y-Nd-Zn-Zr [30], Mg-4Zn-0.5Zr (wt.%) [31], Mg-Zn-Zr, Mg-Ca-Zn-Zr [32], Mg-Gd-Zn-Zr [32], and Mg-Nd-Zn-Zr alloys [32]. Gao *et al*. [32] observed that the Zn-Zr precipitates normally exhibited a rod-shape and are heterogeneously distributed inside individual α-Mg grains. Furthermore, Li *et al.* [33] observed triangular-shaped ZnZr phase and rectangular-shaped Zn_2Zr phase for a Mg-5Zn-2Gd-0.4Zr (wt.%) alloy. Moreover, no relationship between the axes of the rods and the α-Mg matrix seem to exist. The enrichment of Zn and Zr inside the α-Mg matrix, especially in the regions where the precipitates are located, indicates that Zn-Zr precipitates are very likely to be formed during the performed solution treatment of the ZK40 and modified ZK40 alloys. The EDXS~~EDXS~~ line scans show ~~an anti-segregation~~a depletion behaviour for the investigated alloys, in which there is a depletion of Zr and especially Zn near the grain boundaries. This

seems to be a precipitate-free region. After this ‘precipitate-free zone’ there is the formation of a region with small precipitates for the ZK40-Nd and ZK40-Y alloys. This behaviour is not observed for the ZK40-CaO, where only one characteristic region containing precipitates is observed. Regarding the region close to the grain boundary, the precipitates distribution and size seem to follow the same ~~feature~~ behaviour of the ZK40-Nd and ZK40-Y for the heat treatment performed at 475 °C for 24 h for the ZK40-Gd, whereas coarse and sparsely distributed precipitates are formed for the solution treatment performed at 445 °C for 24 h for the ZK40-Gd. In the interior of the grains, the precipitates seem to be arranged in agglomerate lines with a precipitate-free zone around these lines.

The impact of the formation of these coarse precipitates on the ageing behaviour was also investigated by comparing the ageing behaviour of the solution treated alloys to the as-cast material. In the as-cast condition, the amount of Zn, Ca or RE elements in the α-Mg matrix is smaller compared to the solution treated condition (which is expected to be in supersaturated solid solution (SSSS) condition). However, the formation of the precipitates within the grains might lead that SSSS condition does not occur. The ~~anti-segregation~~depletion of Zr and Zn suggest that these elements were consumed for the formation of the precipitates during solution treatment.

The hardness evolution for the T5 and T6 conditions are exhibited in Figure 8. Apart from the ZK40-Gd T6 aged at 200 °C, ZK40-Nd T6 aged at 200 °C and ZK40-Y T6 aged also at 200 °C, a notable ageing behaviour tendency for the modified ZK40 alloys is not observed. Thus, the results here show that the mechanical behaviour within certain ZK40 and ZK40-modified alloys seem to be affected by the formation of precipitates. ~~formation of the precipitates for the ZK40 and ZK40-modified alloys during solution treatment seem to have affected their ageing behaviour.~~ The increase of the hardness for the T6-200°C for the ZK40-Gd, ZK40-Nd and ZK40-Y, though, indicates that precipitates containing RE can form at this temperature, despite the depletion of Zn in the α-Mg matrix.

Conclusion

As-cast ZK40 alloys, modified with the addition of CaO, Gd, Nd and Y were investigated. Solution treatments were performed based on the ~~DTA~~ differential thermal analysis data and the microstructure was analysed by means of SEM and energy dispersive X-ray spectroscopy~~EDXS~~-SEM. The ageing response was monitoring using hardness Vickers.

The following points can be made:

- The as-cast microstructure was modified by the solution heat treatment. The intermetallic compounds were partially dissolved and precipitates were found within the grains;
- An enrichment of Zn and Zr is observed within the grains, especially in the region containing precipitates. According to the literature, it is assumed that they are Zn-Zr precipitates;
- ~~The ageing response of the alloys was significantly low.~~ The highest ageing responses were observed for~~Apart from~~ the ageing at 200 °C performed after solution heat treatment (T4) for the ZK40-Gd, ZK40-Nd and ZK40-Y~~,~~ ~~t~~The other investigated alloys and for the other ageing temperatures the ageing response was ~~do not exhibit~~ less ~~a~~ notable ~~ageing response~~.

References

[1] Kainer, K.U. (Ed.). Magnesium alloys and technology, 2003.

[2] He, S.M.; Peng, L.M; Zeng, X.Q.; Ding, W.J.; Zhu, Y.P.: Mater. Sci. Eng., A. 433, (2006), 175-181.

[3] Roberts, C.S. Magnesium and its Alloys, 1960 Wiley.

[4] Wu, A.; Xia, C.; Wang, J.: Journal of University of Science and Technology Beijing, Mineral, Metallurgy, Material. 13 (2006) 5, 424-428.

[5] Susuki, A.; Saddock, N.D.; TerBush, J.R.; Powell, B.R.; Jones, J.W.; Pollock, T.M.: Metall. Mater. Trans. A. 39 (2008) 3, 696-702.

[6] Hofstetter, J.; Rüedi, S.; Baumgartner, I.; Kilian, H.; Mingler, B.; Povoden-Karadeniz, E.; Pogatscher S.; Uggowitzer, P.J.; Löffler, J. F.: Acta Mater. 98 (2015) 423-432.

[7] Chino, Y.; Ueda, T.; Otomatsu, Y.; Sassa, K.; Huang, X.; Suzuki, K.; Mabuchi, M.: Materi. Trans. 52 (2011) 7, 1477-1482.

[8] Zhang, B.; Wang, Y.; Geng, L.; Lu, C,: Mater. Sci. Eng., A. 539 (2012) 56-60.

[9] Geng, L.; Zhang, B.P.; Li, A.B.; Dong, C.C.: Mater. Lett. 63 (2009) 5, 557-559.

[10] Somekawa, H.; Mukai, T,: Mater. Sci. Eng., A. 459 (2007) 1, 366-370.

[11] Wiese, B.; Mendis, C. L.; Tolnai, D.; Stark, A.; Schell, N.; Reichel, H.-P.; Brückner R.; Kainer K.U.; Hort, N.: J. Alloys Compd. 618 (2015) 64-66.

[12] Hradilová, M.; Vojtěch, D.; Kubásek, J.; Čapek, J.; Vlach, M.: Mater. Sci. Eng., A. 586 (2013) 284-291.

[13] Gao, X.; He, S. M.; Zeng, X. Q.; Peng, L. M.; Ding, W. J.; Nie, J. F.: Mater. Sci. Eng., A. 431 (2006) 1, 322-327.

[14] Honma, T.; Ohkubo, T.; Hono, K.; Kamado, S.: Mater. Sci. Eng., A. 395 (2005) 1, 301-306.

[15] Nie, J.F.; Muddle, B.C.: Acta Mater. 48 (2000) 8, 1691-1703.

[16] Antion, C.; Donnadieu, P.; Perrard, F.; Deschamps, A.; Tassin, C.; Pisch, A.: Acta Mater. 51 (2003) 18, 5335-5348.

[17] Apps, P. J.; Karimzadeh, H.; King, J. F.; Lorimer, G. W.: Scripta Mater. 48 (2003) 8, 1023-1028.

[18] Anyanwu, I. A.; Kamado, S.; Kojima, Y.: Mater. Trans. 42 (2001) 7, 1206-1211, 2001.

[19] Agnew, S. R.; Yoo, M. H.; Tome, C. N.: Acta Mater. 49 (2001) 20, 4277-4289.

[20] Agnew, S.R.; Senn, J.W.; Horton, J.A.: Jom. 58 (2006) 5, 62-69.

[21] Datta, A.; Waghmare, U.V.; Ramamurty, U.: Acta Mater. 56 (2008) 11, 2531-2539.

[22] Gao, L.; Chen, R. S.; Han, E.H.: J. Alloys Compd. 472 (2009) 1, 234-240.

[23] Suzuki, M.; Kimura, T.; Koike, J.; Maruyama, K.: Mater. Sci. Eng., A. 387 (2004) 706-709.

[24] Suzuki, M.; Maruyama, K.: In: Materials Science Forum. Trans Tech Publications, 2010, 1602-1607.

[25] Rokhlin, L.L.: Magnesium alloys containing rare earth metals: structure and properties, 2003, Crc Press.

[26] Honma, T.; Ohkubo, T.; Kamado, S.; Hono, K.: Acta Mater. 55 (2007) 12, 4137-4150.

[27] He, S. M.; Peng, L. M.; Zeng, X. Q.; Ding, W. J.; Zhu, Y. P.: Mater. Sci. Eng., A. 433 (2006) 1, 175-181.

[28] Luo, J.; Ying, K.; He, P.; Bai, J.: Digit. Signal Process. 15 (2005) 2, 122-136.

[29] Horie, T.; Iwahori H.; Seno, Y.; Awano, Y.: Development of high creep-resistant magnesium alloy strengthened by Ca addition, in Magnesium Technology 2000, Y. Kojima, T. Aizawa and S. Kamado, eds., TMS, Warrendale, 2000, 261.

[30] Morgan, J.E.; Mordike, B.L.: Development of creep resistant magnesium rare earth alloys, in Strength of Metals and Alloys (ICSMA6, Melbourne, Australia 1982), R.C. Gifkins, ed., Pergamon Press, Oxford, 1983, 643.

[31] Bettles, C.J.; Gibson, M.A.; Venkatesan, K.: Scripta Mater. 51 (2004) 193.

[32] Gao, X.; Muddle, B.C.; Nie, J.F.: Philos. Mag. Lett. 89 (2009) 1, 33-43.

[33] Li, J.H., Barrirero, J., Sha, G., Aboulfadl, H., Mücklich, F., Schumacher, P.: Acta Mater. 108 (2016) 207-218.

Ricardo Henrique Buzolin

Formatted: Font: Arial, English (United Kingdom)

Formatted: Font: Arial, English (United Kingdom)

Formatted: Normal, Justified, Line spacing: Double

Formatted: Default Paragraph Font, Font: Arial, English (United Kingdom)

Formatted: Font color: Auto, English (United Kingdom), Pattern: Clear

Formatted: Font color: Auto, English (United Kingdom), Pattern: Clear

Formatted: Font color: Auto, English (United Kingdom), Pattern: Clear

Diploma in Mechanical Engineering from the University of Sao Paulo, Brazil. Master in Materials Science and Engineering from the University of Sao Paulo about corrosion and mechanical properties of magnesium alloys. Since 2016 PhD student at Graz University of Technology with the topic of thermomechanical treatment and modelling of titanium alloys.

Tables and Figures

Table 1: Chemical compositions of the investigated alloys measured with X-ray fluorescence (Gd and Zn) and spark analyser (Ca, Cu, Fe, Nd, Ni, Y, Zr).

Alloys	Zn %wt	Zr %wt	Ca %wt	Y %wt	Fe (ppm)	Cu	Ni (ppm)
ZK40	5.00	0.53	-	-	11.3	14.1	12.8
ZK40-CaO	4.385	0.34	1.22	-	13.5	16.4	14.1
ZK40-Gd	4.50	0.55	1.70	-	6.9	29.2	<30
ZK40-Nd	4.70	0.55	-	2.46	11	14.8	28.2
ZK40-Y	4.10	0.33	-	1.12	3.8	29	<2

Table 2: Solution treatment temperatures that were used in this investigation.

Alloy	Solution treatment temperature

ZK40	320 °C
ZK40-CaO	370 °C
ZK40-Gd	445 °C, 475 °C
ZK40-Nd	440 °C, 475 °C
ZK40-Y	480 °C

Table 3: Differential temperature analysis temperatures for the exothermic reactions associated to the formation of α-Mg (Mg) and intermetallic compounds (IC) during cooling.

~~DTA~~ Differential thermal analysis temperatures formation during cooling (°C)		
ZK40		
IC1		Mg
337.7 ± 0.1		638.5 ± 0.1
ZK40-CaO		
IC1		Mg
390.0 ± 0.5		631.4 ± 0.1
ZK40-Gd		
IC1		Mg
496.4 ± 1.5		636.2 ± 0.1
ZK40-Nd		
IC1	IC2	Mg

466.3 ± 0.4	487.8 ± 0.5	638.0 ± 0.2
ZK40-Y		
IC1		Mg
499.3 ± 2.9		638.2 ± 0.2

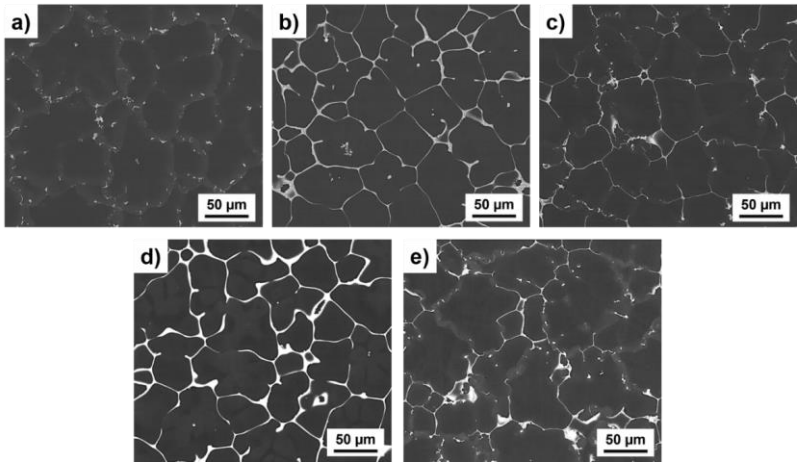

Figure 1: SEM micrographs of the as-cast alloys: a) ZK40; b) ZK40-CaO; c) ZK40-Gd; d) ZK40-Nd; e) ZK40-Y.

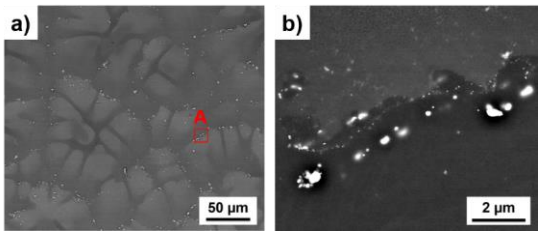

Figure 2: SEM micrographs of the solution heat treated ZK40 alloy at 320 °C for 24 h: a) general representative view; b) Region A highlighting the formation of precipitates at the grain boundaries and small precipitates within the α-Mg matrix.

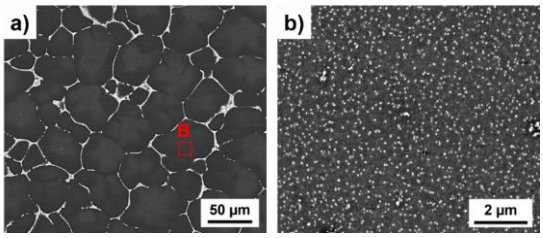

Figure 3: SEM micrographs of the solution heat treated ZK40-CaO alloy at 370 °C for 24 h: a) general representative view of the solution treated microstructure; b) Region B highlighting the formation of precipitates within the α-Mg matrix.

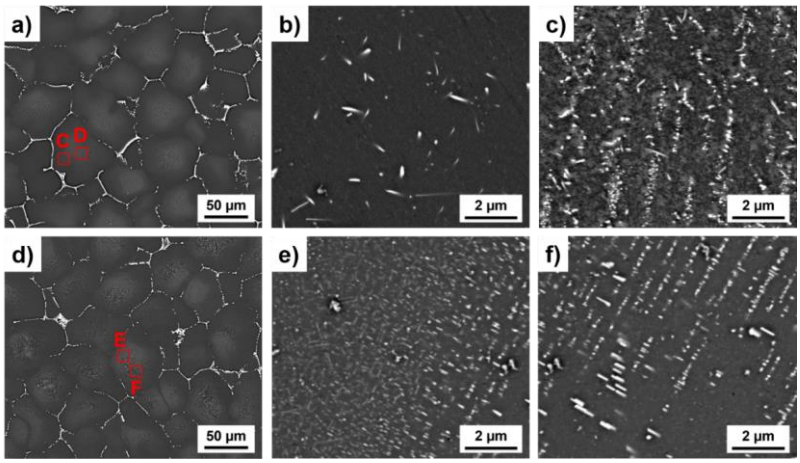

Figure 4: SEM micrographs of the solution heat treated ZK40-Gd alloy: (a,b,c) at 445 °C for 24 h and (d,e,f) 475 °C for 24 h. a,d) general representative view of the solution treated microstructure; b,e) Region C and E, respectively, highlighting the formation of precipitates in a region near the grain boundary; c,f) Region D and F, respectively, highlighting the formation of precipitates in the middle of the α-Mg grain.

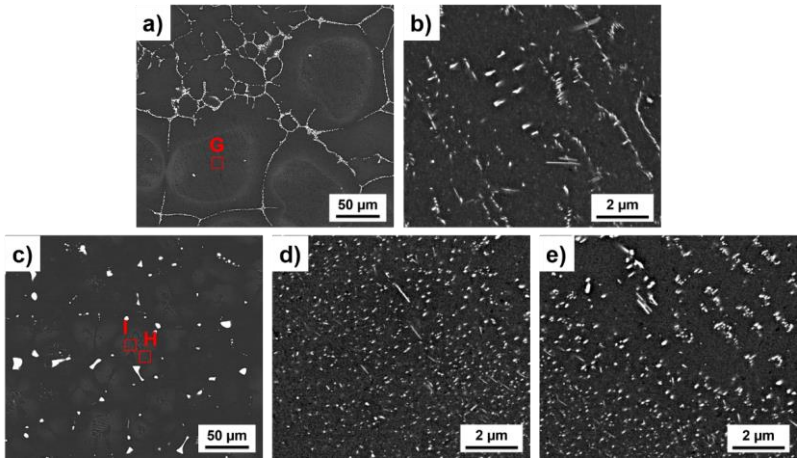

Figure 5:SEM micrographs of the solution heat treated ZK40-Nd alloy: (a,b) at 440 °C for 24 h and (c,d,e) 475 °C for 24 h. a,c) general representative view of the solution treated microstructure; b) Region G, highlighting the formation of the representative precipitate-zone for the solution treatment performed at 440 °C; d) Region H, highlighting the formation of precipitates in a region near the grain boundary; e) Region I, highlighting the formation of precipitates in the middle of the α-Mg grain.

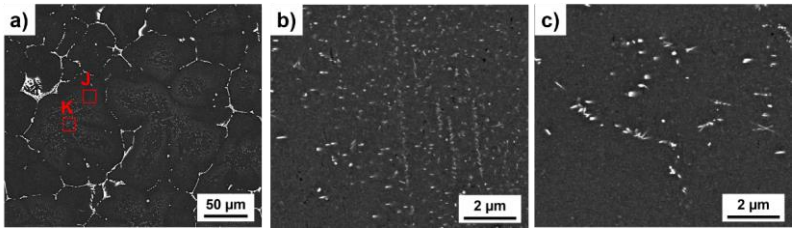

Figure 6: SEM micrographs of the solution heat treated ZK40-Y alloy at 480 °C for 24 h: a) general representative view of the solution treated microstructure; b) Region J, highlighting the formation of precipitates in a region near the grain boundary; c) Region K, highlighting the formation of precipitates in the middle of the α-Mg grain.

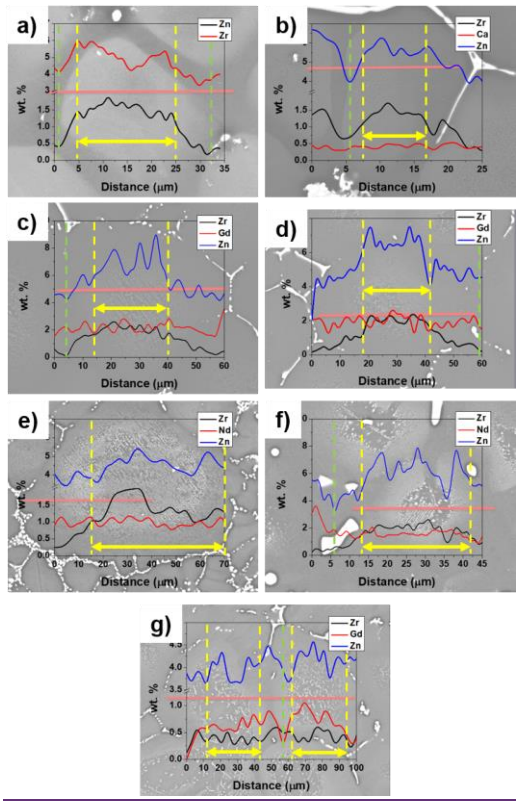

Figure 7: Energy dispersive X-ray spectroscopy line scans for the solution treated alloys: a) ZK40 after solution treatment at 320 °C for 24 h; b) ZK40-CaO after solution treatment at 370 °C for 24 h; c) ZK40-Gd after solution treatment at 445 °C for 24 h; d) ZK40-Gd after solution treatment at 475 °C for 24 h; e) ZK40-Nd after solution treatment at 440 °C for 24 h; f) ZK40-Nd after solution treatment at 475 °C for 24 h; g) ZK40-Y after solution treatment at 480 °C for 24 h. The yellow dashed lines and arrows indicate the regions of the precipitates. The grain boundaries are indicated in green dashed lines.

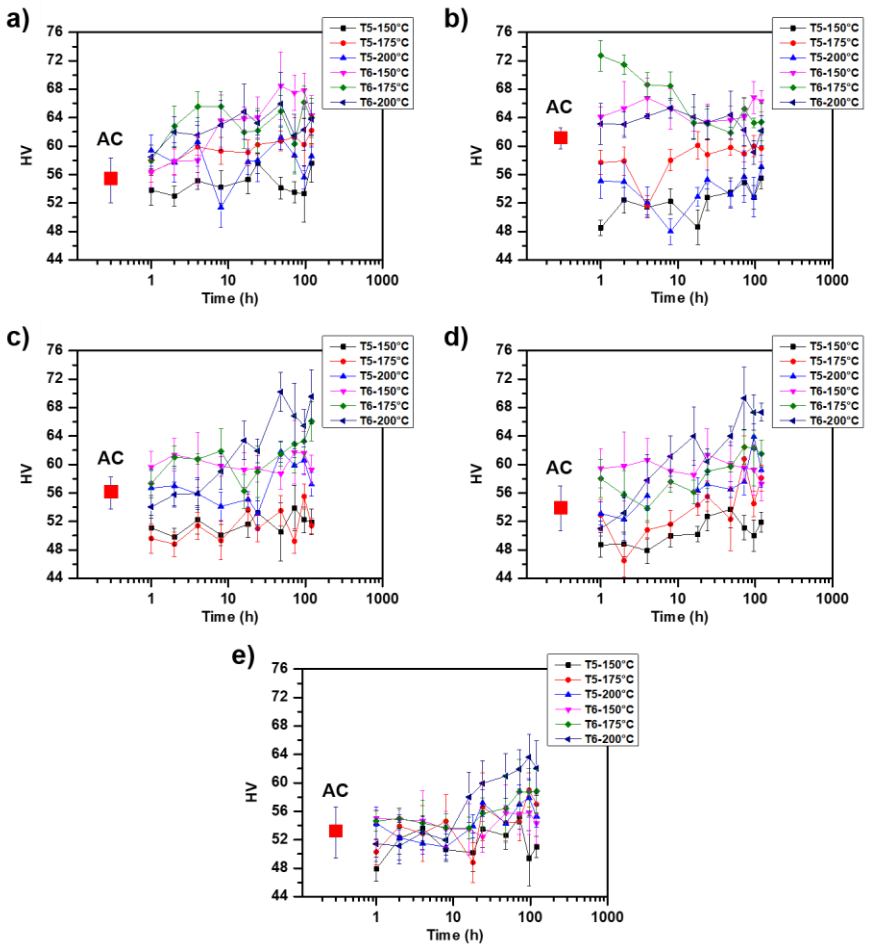

Figure 8: Hardness evolution for the ageing heat treatments performed after solution treatment (T6) and for the as-cast material (T5): a) ZK40 alloy; b) ZK40-CaO alloy; c) ZK40-Gd alloy; d) ZK40-Nd; e) ZK40-Y.

Formatted: English (United Kingdom)